Electronic structure and optical properties of the red and yellow mercuric iodides*

Xu Bin(徐 斌)† and Lü Jian(吕 健)

Department of Mathematics and Information Sciences, North China Institute of Water Conservancy and Hydroelectric Power, Zhengzhou 450011, *China*

(Received 24 April 2009; revised manuscript received 15 September 2009)

With the help of the *ab initio* full-potential linearized augmented plane wave (FPLAPW) method, calculations of the electronic structure and linear optical properties are carried out for red HgI_2 and yellow HgI_2. It is found that the red HgI_2 has a direct gap of 1.22834 eV and the yellow HgI_2 has an indirect gap of 2.11222 eV. For the red HgI_2, the calculated optical spectra are qualitatively in agreement with the experimental data. Furthermore, the origins of the different peaks of $\varepsilon_2(\omega)$ are discussed. Our calculated anisotropic dielectric function of the red HgI_2 is a nice match with the experimental results. Our calculated results are able to reproduce the overall trend of the experimental reflectivity spectra. Although no comparable experimental and theoretical results are available, clearly, the above proves the reliability of our calculations, suggesting that our calculations should be convincing for the yellow HgI_2. Finally, the different optical properties are discussed.

Keywords: *ab initio*, electronic band structure, optical properties, semiconductor
PACC: 7115A, 7125, 7820D, 7850G

1. Introduction

In the past several decades there has been a renewed interest in mercuric iodide (HgI_2) in order to obtain further knowledge about its structure and physical properties. Single crystals of the tetragonal form of mercuric iodide (HgI_2) have important applications as photocells, x-ray and γ-ray radiation detectors, due to the large band gap, high resistivity, large (average) atomic mass, and the acceptable mobilities and lifetimes of both electrons and holes.[1−6] It has an advantage over the more commonly used silicon and germanium detectors in that, with its larger band gap, it can be operated at room temperature. Much research work has been done on the various aspects of the optical and electric transport properties.[7−11] Besides these useful properties, however, there are found some disadvantages with HgI_2, such as the problems associated with the small hole mobility (at room temperature and along the c axis)[12,13] and the fact that HgI_2 has a high vapour pressure, which means that the crystal should not be exposed to vacuum during measurements.

In recent years, many experimental and theoretical methods have been applied to the study of mercuric iodide (HgI_2), thereby greatly expanding and deepening our understanding of its structural and physical properties. Gonzalez and Ibarra[14] measured the effect of small deformations on the optical properties of HgI_2 qualitatively. Yao *et al.*[15] studied the anisotropic optical properties of the HgI_2 crystal, by variable angle spectroscopic ellipsometry. Tyagi and Vedeshwar[16] studied the thin film growth of HgI_2 systematically by using structural, compositional, morphological, and optical absorption analyses. Alexander *et al.*[17] investigated bulk-grown HgI_2 crystals. Turner and Harmon[18] calculated the self-consistent, relativistic electronic structure of tetragonal mercuric iodide. Chang and James[19] presented empirical nonlocal pseudopotential calculations of the electronic band structure of undoped mercuric iodide in its red tetragonal form. Values for the electron and hole effective masses, optical matrix elements for interband transitions, and complex dielectric function have been reported. The excitonic effects on the absorption coefficient near the fundamental band gap were taken into account in the effective-mass approximation. *Ab initio* methods were applied to HgI_2, PtI_2, and PbI_2 to assess the effect of relativistic effective core potentials on ground-state properties of heavy-metal iodides.[20] Ahuja *et al.*[21] used the linear muffin-tin orbital method, within the local-density ap-

*Project supported by Program for Science and Technology Innovation Talents in Universities of Henan Province, China (Grant No. 2008HASTIT008), the National Natural Science Foundation of China (Grant No. 10574039) and the Key Project Foundation of Science and Technology of He'nan Province, China (Grant No. 092102210166).
†Corresponding author. E-mail: hnsqxb@163.com
© 2010 Chinese Physical Society and IOP Publishing Ltd

proximation and without geometrical approximations, to calculate the electronic structure of red HgI_2. Using the self-consistent potential, they calculated the energy bands and from these the anisotropic frequency-dependent dielectric function and the reflectivity spectrum were derived. Ortega *et al.*[22] reported on the density of states of mercuric iodide calculated by using the recursion method. Ayres *et al.*[23,24] investigated the structural and electronic properties and the role of intrinsic defects in the electronic and optical properties of mercuric iodide in the red tetragonal crystalline phase by using the *ab initio* method.

The aim of this paper is to present the results of the theoretical investigation of the electronic energy band, total and partial densities of states (DOS) and optical properties for the red HgI_2 and yellow HgI_2, based on the full potential linearized augmented plane wave (FPLAPW) method. Furthermore, the results of the present calculations are used to explain some aspects of the previous experimental and theoretical results.

2. Computational details

The geometry optimization and the electronic structure calculations for the red HgI_2 and the yellow HgI_2 are carried out by using the FPLAPW method implemented in the WIEN2K package.[25] The generalized gradient approximation (GGA) in the scheme of Perdew, Burke, and Ernzerhof[26] (PBE) is used for the exchange–correlation functional, and the relativistic effects are taken into account in the scalar approximation. We take RmtKmax to be 8.5 and make the expansion up to $l = 10$ in the muffin tins. The use of the full-potential ensures that the calculation is completely independent of the choice of the sphere radii. Nonoverlapping MT sphere radii of 2.5 and 2.3 a.u. are used for Hg and I atoms, respectively. We use 14×14×4 (15×15×4) meshes for the red (yellow) HgI_2, which represent 1000 k-points in the first Brillouin zone. Self-consistency is considered to be achieved when the total energy difference between succeeding iterations is less than 10^{-5} Ry per formula unit.

The imaginary part of the dielectric tensor is directly related to the electronic band structure of a solid, so it can be computed from knowledge of the single-particle orbitals and energies approximated by the solutions of the Kohn–Sham equations. Assuming the one-electron rigid band approximations, neglecting electron polarization effects (Koopmans' approximation) and in the limit of linear optics and of the visible–ultraviolet region,[27,28] the imaginary part of a matrix element of the dielectric tensor is given by

$$\varepsilon_2(\omega) = \frac{4\pi^2 e^2}{m^2\omega^2} \sum_{i,f} \int_{\mathrm{BZ}} \frac{2\mathrm{d}\boldsymbol{k}}{(2\pi)^3} \left|\langle\varphi_{f\boldsymbol{k}}| e\cdot p |\varphi_{i\boldsymbol{k}}\rangle\right|^2 \times \delta(E_f(\boldsymbol{k}) - E_i(\boldsymbol{k}) - \hbar\omega) \quad (1)$$

for a vertical transition from a filled initial state $|\varphi_{i\boldsymbol{k}}\rangle$ of energy $E_i(\boldsymbol{k})$ to an empty final state $|\varphi_{f\boldsymbol{k}}\rangle$ of energy $E_f(\boldsymbol{k})$, with wave vector $\boldsymbol{k}$. ω is the frequency, e the electron charge, m the free electron mass, and p the momentum operator.

By using the well-known Kramers–Kronig transformation, the real parts of the dielectric function can be related to its imaginary parts $\varepsilon_2(\omega)$. In the tetragonal (orthogonal) phase, $\varepsilon(\omega)$ is anisotropic and has two (three) different fractions, $\varepsilon_{xx}(\omega)$ and $\varepsilon_{zz}(\omega)$($\varepsilon_{xx}(\omega)$,$\varepsilon_{yy}(\omega)$ and $\varepsilon_{zz}(\omega)$), respectively. We present an average over the two (three) components as $[2\varepsilon_{xx}(\omega) + \varepsilon_{zz}(\omega)]/3$($[\varepsilon_{xx}(\omega) + \varepsilon_{yy}(\omega) + \varepsilon_{zz}(\omega)]/3$) for the tetragonal (orthogonal) phase. Using the $\varepsilon(\omega)$ (where $\varepsilon(\omega) = \varepsilon_1(\omega) + \mathrm{i}\,\varepsilon_2(\omega)$) as output, we calculate various optical constants,[29] such as spectral reflectivity $R(\omega)$, absorption coefficient $I(\omega)$, electron energy loss function $L(\omega)$, real part $n(\omega)$, and imaginary part $k(\omega)$ of the refractive index with a simple independent program.[29]

3. Results and discussion

We first give the results of the total energy as a function of volume per formula unit for the red and yellow HgI_2 compounds in Fig. 1. Table 1 presents the calculated equilibrium lattice constants for the red HgI_2 and the yellow HgI_2 that are determined by fitting the total energy as a function of volume to the Murnaghan equation of state.[30] We have an overestimate of equilibrium lattice constants for the red HgI_2 and the yellow HgI_2 that are determined by fitting the total energy as a function of volume to the Murnaghan equation of state.[30] We have an overestimate of the lattice constants which are 3.41% and 2.74% (3.51% and 3.34%) more than the experimental values in Ref. [31] (Ref. [32]) for the red HgI_2 and the yellow HgI_2 respectively.

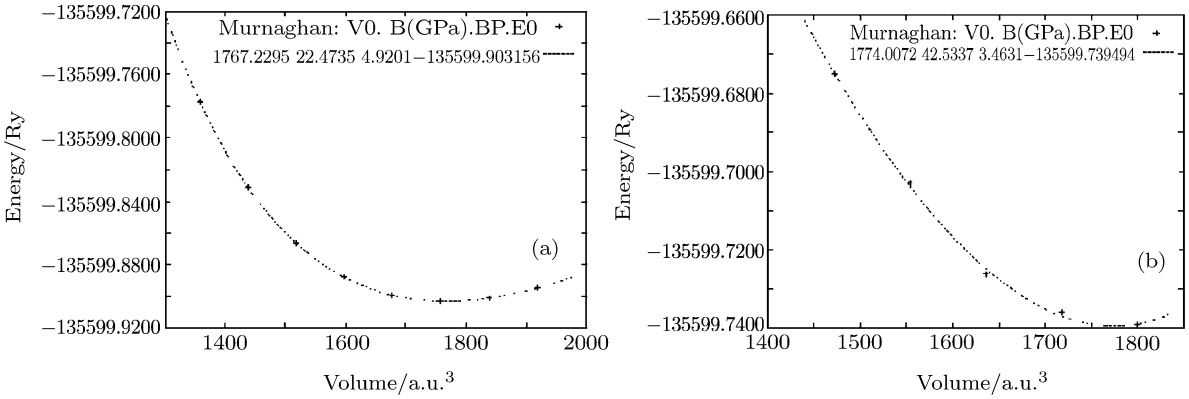


Fig. 1. Total energies as a function of volume of (a) the red HgI_2, and (b) the yellow HgI_2.

Table 1. Values of lattice constant, volume equilibrium, bulk modulus B_0 and its first derivative B_0' and calculated GGA bandgaps (in eV) of the red and yellow HgI_2 compounds compared with other theoretical and experimental results. (1 Å=0.1 nm)

		a/Å	b/Å	c/Å	V/Å^3	B_0/GPa	B_0'	bandgaps/eV
Hg(red)	this work	4.5099	4.5099	12.8751	1767.2295	22.4735	4.9201	1.22834
	Exp.	4.361[a]		12.45[a]	1597.8597[a]			2.29[e],
		4.357[b]		12.36[b]				2.14[f]
other calc.								2.37[c], 1.1[d]
Hg(yellow)	this work	4.8309911	7.6359	14.2526	3548.0144	42.5337	–3.4631	2.11222
	Exp.	4.702[a]	7.432[a]	13.872[a]	3271.3314[b]			3.05[e]
		4.674[b]	7.32[b]	13.76[b]	3167.9863[b]			

[a] Ref. [31]. [b] Ref. [32]. [c] Ref. [19]. [d] Ref. [21]. [e] Ref. [7]. [f] Ref. [33].

Band dispersions for the red HgI_2 and the yellow HgI_2 calculated by DFT within GGA at equilibrium lattice constants are presented in Fig. 2. The general features of the band dispersions accord with the previous results [18,19,34]. It is found that the red HgI_2 is a direct band gap semiconductor due to the fact that the top of the valence bands and the bottom of the conduction bands are at the same Γ-point. The most prominent features of the calculated band structures (bandgaps) of the red HgI_2 and the yellow HgI_2 are listed in Table 1. We obtain a direct gap of 1.22834 eV for the red HgI_2, in agreement with other results of Ahuja *et al.*,[21] who used the linear muffin-tin orbital method. Turner and Harmon[18] used the Korringa–Kohn–Rostoker (KKR) method to obtain a gap of 0.52 eV, while Chang and James[19] empirically adjusted the gap to the experimental value. For the yellow HgI_2, the calculated band gap of 2.11222 eV is indirect. The bottom of the conduction band (CB) is at the H point and the top of the valence band (VB) is at the Γ point.

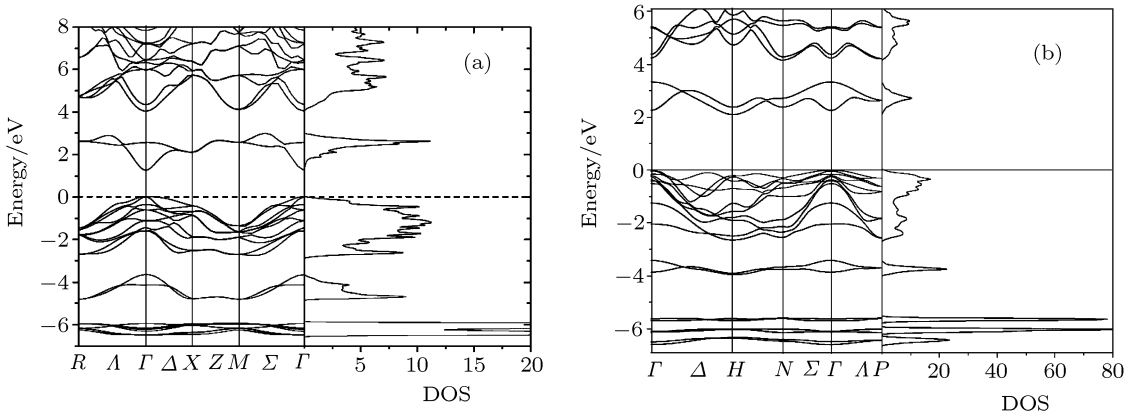


Fig. 2. Band structures for (a) the red HgI_2 and (b) the yellow HgI_2. The horizontal dashed line indicates the Fermi level at 0 eV.

This underestimation of the t band gaps is mainly due to the fact that the simple form of DFT does not take into account the quasiparticle self energy correctly[35] which makes it not sufficiently flexible to accurately reproduce both exchange correlation energy and its charge derivative. It is important to note that the density functional formalism is limited in its validity[36] and the band structure derived from it cannot be used directly for comparison with experiment.

Figure 3 shows the partial DOSs of the red HgI_2 and the yellow HgI_2. There are some bands around -6 eV in Figs. 2 (a) and 2(b). It can be assessed that these bands consist of Hg d and I f orbitals. The very small dispersions of these bands imply their localized character. The two bands around -4.2 eV of the red HgI_2 are valence bands that are composed mainly of 6s, 5d states of the Hg atom and 5p states of the I atom. Furthermore, the two bands around -3.8 eV of the yellow HgI_2 are valence bands that are composed mainly of 6s, 5d states of the Hg atom and 5s states of the I atom. The next higher bands of the red HgI_2, ranging from about -2.9 eV up to the Fermi level, are valence bands that are formed mainly by 6p, 5d states of the Hg atom and 5p states of the I atom, while the next higher bands of the yellow HgI_2, ranging from about -2.9 eV up to the Fermi level, are valence bands that are composed mainly of 6p, 5d states of the Hg atom and 5s, 4d states of the I atom. The conduction bands of the red HgI_2 are composed mainly of 6s, 5p states of the Hg atom and 5p states of the I atom, and the conduction bands of the yellow HgI_2 are formed mainly by 6s, 5p states of the Hg atom and 5s, 4d states of the I atom.

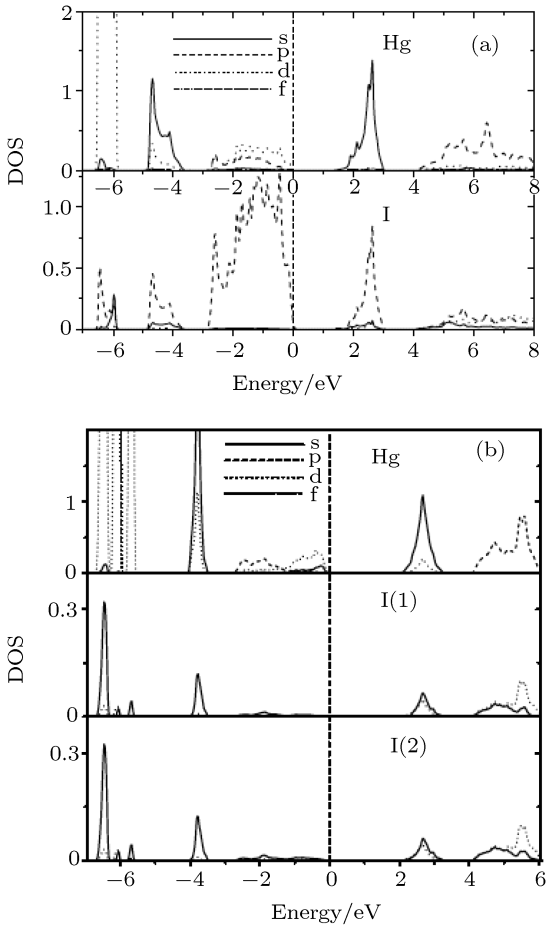


Fig. 3. Partial density of states (PDOS) of the red HgI_2 and (b) the yellow HgI_2. The vertical dashed line indicates the Fermi level at 0 eV.

It has been earlier found that the calculated optical properties for $Zn_{1-x}Co_xX$ (X=S, Se, Te),[37] Fe nanowires on Cu(001) and Ag(001),[38] $Ba_{0.5}Sr_{0.5}TiO_3$,[39] Cu-doped AlN[40] and TiO_2 [41] accord well with the experimental findings, and we therefore use the same theory to predict the optical properties of the red HgI_2 and the yellow HgI_2. Because of the underestimation of the optical band gaps in the DFT calculations, the locations of all the peaks in the spectral profiles are consistently shifted toward lower energies as compared with the experimentally determined spectra. Rigid shift (by the scissor operator) of the optical spectra is applied, which somewhat reduces the discrepancy between the theoretical and experimental results.

Figure 4 shows the calculated values of $\varepsilon_2(\omega)$ for the red HgI_2 and the yellow HgI_2 along with the available experimental results[42] up to a photon energy of 20 eV. The calculated spectra have been scissor-shifted by an amount equal to the difference between the calculated and the experimental band gaps (1.103 eV for the red HgI_2 [33] and 0.93778 eV for the yellow HgI_2[7]). For the red HgI_2, the calculated optical spectra agree with the experimental data qualitatively.[42] In our calculations, the intensities of the major peaks are underestimated, while the intensities of some of the shoulders are overestimated. This result is consistent with the previous theoretical findings.[21] For the yellow HgI_2, we do not find any experimental data or theoretical calculations to be compared with our results. For the red HgI_2, the peak A mainly comes from the electron transition from I 5p (VB) to Hg 6s (CB) orbitals. The peaks B, C, D and E originate mainly from the transition between the I 5p (VB) and Hg 6s, 5d (CB) orbitals, and the peak F comes mainly from the transition between the I 5s, 5p (VB) and Hg 5p, 5d (CB) orbitals. For the yellow HgI_2, the peak A mainly comes from the electron transition from the I 5s (VB) to Hg 5d, 6s (CB) orbitals. The peaks B and C arise mainly from the transition

between the I 5s (VB) and Hg 6s, 5d (CB) orbitals, and the peaks D, E and F are ascribed mainly to the transition between the I 5s, 5p (VB) and Hg 5p, 5d (CB) orbitals. Furthermore, intra-band transitions also play an important role in producing these peaks. The optical properties of critical peaks are ascribed to the transitions of inner electron excitation from near VB semicore states to CB. The optical properties of critical peaks above 12 eV are attributed to the transitions of inner electron excitation from near VB semicore states I 4d, 5s, 5p (VB) and Hg 5p, 5d (CB) levels to CB. It is noted that a peak in $\varepsilon_2(\omega)$ does not correspond to a single interband transition since many direct or indirect transitions may be found in the band structure with an energy corresponding to the same peak.

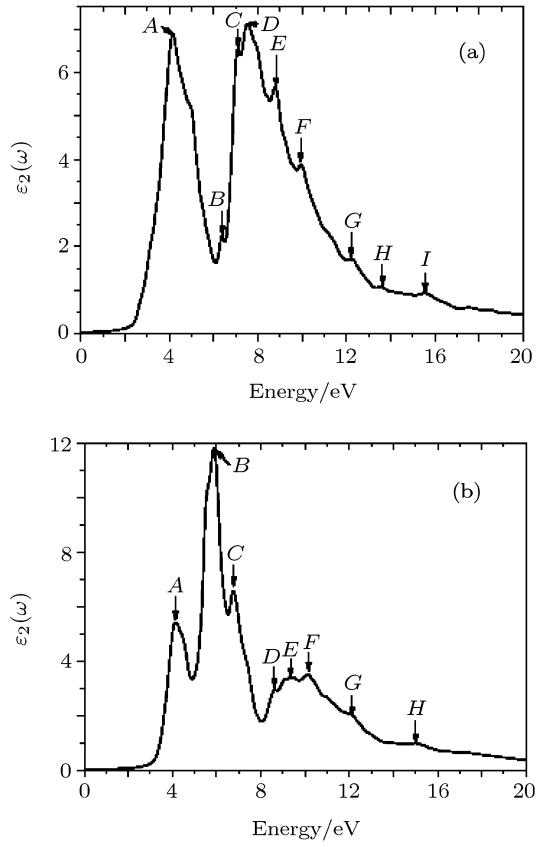


Fig. 4. Imaginary part $\varepsilon_2(\omega)$ of the dielectric function of (a) the red HgI_2, and (b) the yellow HgI_2.

Figure 5 shows the anisotropic dielectric functions of the red HgI_2 crystal in a range of 1–6 eV. Figures 5(a) and 5(b) represent the experimental results[15] and the calculated spectra, respectively. As can be seen in the figure there is a close match between our calculated results and experimental results in the whole energy region, but the locations of the peaks do not coincide with each other. Considering the unreliability of the experimental results due to the high chemical activity of the surface of the red and yellow HgI_2 compounds for chemical adsorption of ambient gas molecules[43] our results need to be reasonably compared with more experimental data in this energy range.

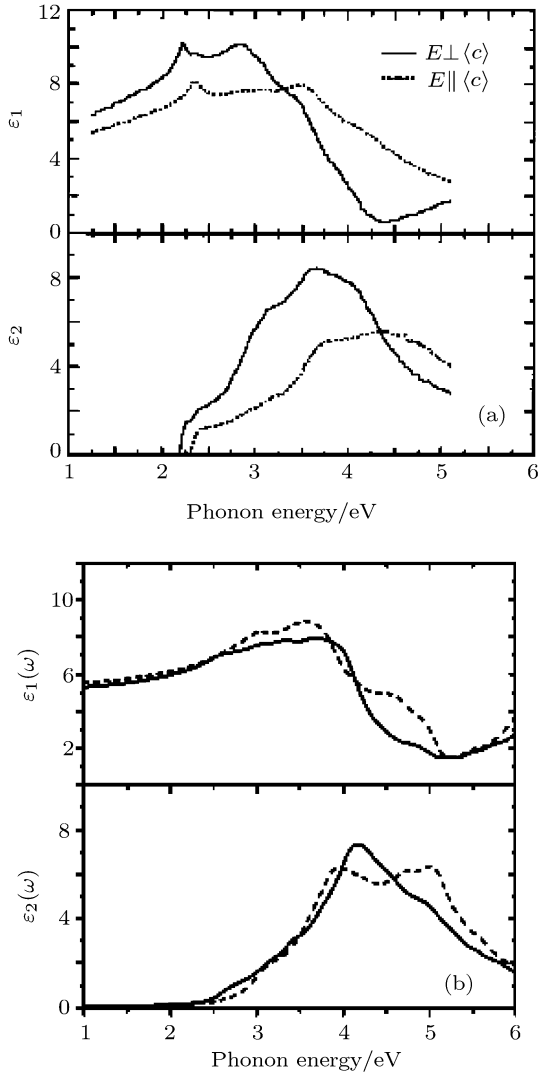


Fig. 5. Anisotropic dielectric functions of the red HgI_2 with ordinary ($E \perp C$) and extraordinary ($E \parallel C$) responses, respectively. (a) represents data taken from the experimental studies by Yao *et al.* (Ref. [15]); (b) represents the calculated reflectivity spectra.

Figure 6 shows the reflectivity spectra for the red HgI_2 and the yellow HgI_2. For the red HgI_2, as can be seen in Fig. 6(a), there is a close match between our calculated results and the experimental results[42] in the whole energy region. However, it should be noted that the difference in high energy between the experimental and theoretical curves can be explained by the fact that DFT allows the calculation of only the ground state, but the experimental results are not obtained from the ground state Although there are

no experimental data or theoretical calculations to be compared with our results, clearly, the above proves the reliability of our calculations, suggesting that calculations should be convincing for the yellow HgI_2 in Fig. 5(b). The good agreement between the theoretical and experimental optical spectra implies that the present calculations are able to well reproduce the other theoretical optical spectra of the red HgI_2 and the yellow HgI_2.

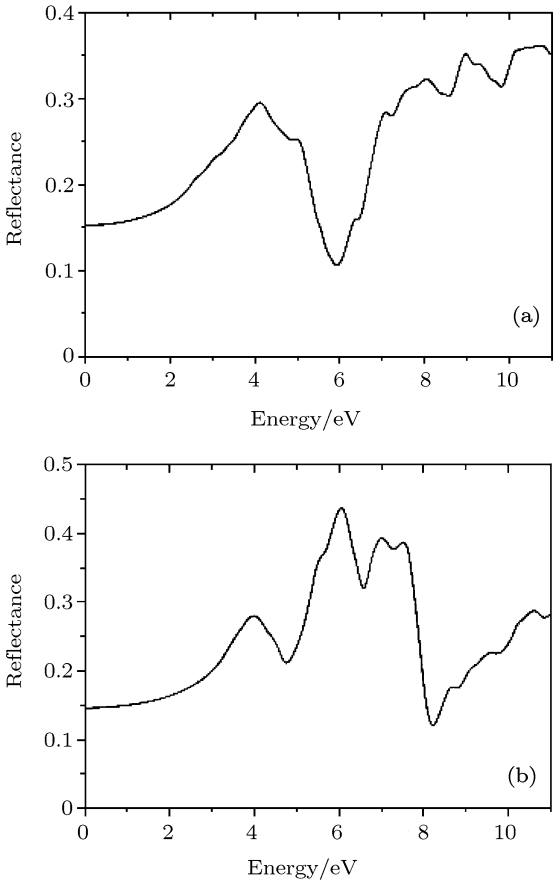


Fig. 6. Reflectivity spectra for (a) the red HgI_2, and (b) the yellow HgI_2.

The imaginary parts of the dielectric function $\varepsilon_1(\omega)$, the absorption coefficient $I(\omega)$, the refractive index $n(\omega)$, the extinction coefficient $k(\omega)$, and the electron energy loss function $L(\omega)$ are plotted in Fig. 7 for the red HgI_2 and the yellow HgI_2. The zeros of $\varepsilon_1(\omega)$ correspond to the local maxima of the extinction coefficient $k(\omega)$, which is shown in Fig. 7. On the other hand, in the energy loss spectra as shown in Fig. 7, we do not find any distinct maxima at energies smaller than 20 eV. The reason for this is that $\varepsilon_2(\omega)$ is still large at these energy values. At 20.75 eV for the red HgI_2 and at 20.15 eV for the yellow HgI_2, there separately appears a large peak in the energy loss spectra. At such high energies the values of $\varepsilon_2(\omega)$ are small, and thus the energy loss becomes large. The energy of the peak of the electron energy loss function $L(\omega)$ is usually assigned to the energy of the volume plasmon, $\hbar\omega_{\rm p}$.[44] For the yellow HgI_2 the value is about 20.76 eV.

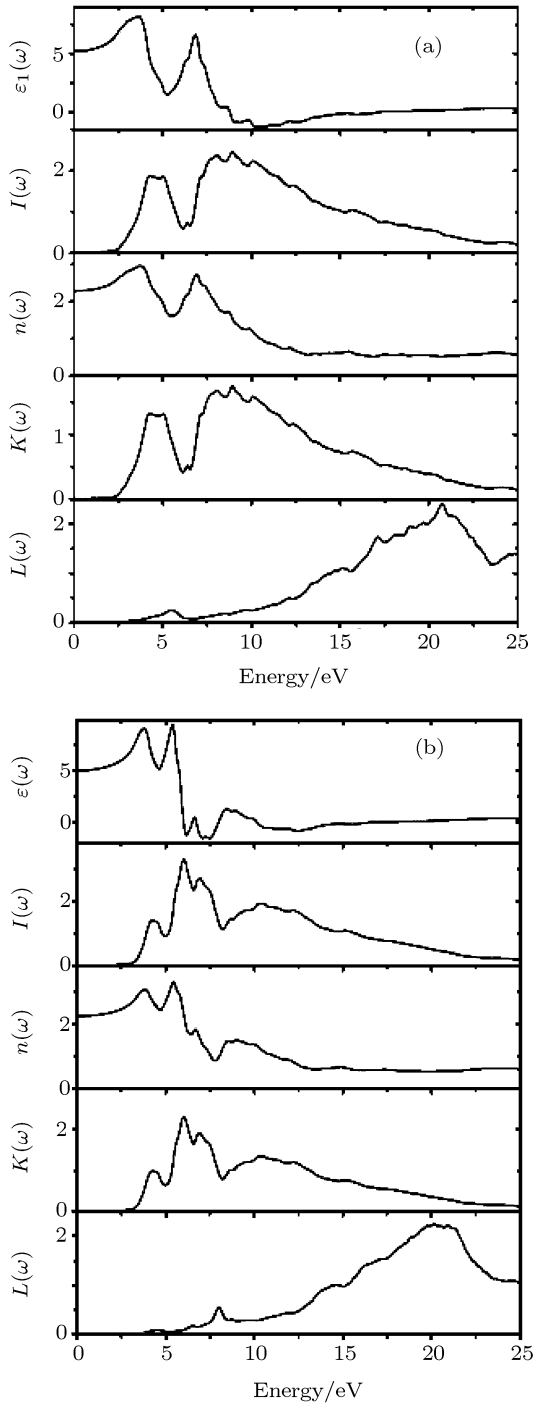


Fig. 7. Frequency dependent optical properties for (a) the red HgI_2 and (b) the yellow HgI_2.

In the yellow HgI_2, because of the absence of a well-defined peak, we assume that the $\hbar\omega_{\rm p}$ lies near 20.5 eV. The other important optical properties calculated in this work are $I(\omega)$ and $K(\omega)$ displayed in

Fig. 7. It is interesting that the profiles of both $I(\omega)$ and $K(\omega)$ are rather similar in shape but different in magnitude. There are sharp peaks in both the energy loss spectra at around 4.28 eV, 5.03 eV, 6.39 eV, 8.03 eV, 8.94 eV and 10.11 eV for $I(\omega)$ and $K(\omega)$ of the red HgI_2 and at around 4.24 eV, 6.02 eV, 6.92 eV and 10.42 eV for $I(\omega)$ and $K(\omega)$ of the yellow HgI_2.

4. Conclusion

We give a more detailed first-principles calculation on the electronic structure and linear optical properties of the red HgI_2 and the yellow HgI_2 by using the FPLAPW method. Electronic energy bands, total and partial densities of states, including optical properties, are analysed. We obtain a direct gap of 1.22834 eV for the red HgI_2 and an indirect gap of 2.11222 eV for the yellow HgI_2. For the red HgI_2, the calculated optical spectra qualitatively accord with the experimental data. Furthermore, the origins of the different peaks of $\varepsilon_2(\omega)$ are discussed. Our calculated anisotropic dielectric function of the red HgI_2 is a nice match with the experimental results. Our calculated results are able to reproduce the overall trend of the experimental reflectivity spectra.[42] Although there are no experimental data or theoretical calculations to be compared with our results, clearly, the above proves the reliability of our calculations, suggesting that calculations should be convincing for the yellow HgI_2. The different optical properties are shown in Fig. 7.

References

[1] Ponpon J P, Stuck R, Siffert P, Meyer B and Schwab C 1975 *IEEE Trans. Nucl. Sci.* **NS-22** 182
[2] Whited R C and Schieber M 1979 *Nucl. Instrum. Methods* **162** 119
[3] Dabrowski A J, Szymczyk W M, Iwanczyk J S, Kusmiss J H, Drummond W and Ames L 1983 *Nucl. Instrum. Methods Phys. Res.* **213** 89
[4] Wong D, Schlesinger T E, James R B, Ortale C, Berg L and Schnepple W F 1988 *J. Appl. Phys.* **64** 2049
[5] Gerrish V and Berg L 1990 *Nucl. Instrum. Methods Phys. Res.* A **294** 41
[6] Burger A, Morgon S H, Silberman E, Nason D and Cheng A Y 1992 *Nucl. Instrum. Methods Phys. Res.* A **322** 427
[7] Bube R H 1957 *Phys. Rev.* **106** 703
[8] Brodin M S, Kadan V N and Matsko M G 1985 *Sov. Phys. Solid State* **27** 477
[9] Tubbs M R 1972 *Phys. Status Solid* B **49** 11
[10] Stuck R, Muller J C, Ponpon J P, Scharager C, Schwab C and Siffert P 1976 *J. Appl. Phys.* **47** 1545
[11] Levi A, Schieber M M and Burshtein Z 1985 *J. Appl. Phys.* **57** 1944
[12] Ottaviani G, Canali C and Quaranta A A 1975 *IEEE Trans. Nucl. Sci.* **NS-22** 192
[13] Minder R, Ottaviani G and Canali C 1976 *J. Phys. Chem. Solids* **37** 417
[14] Gonzalez M and Ibarra A 1995 *Phys. Rev.* B **51** 13786
[15] Yao H, Johs B and James R B 1997 *Phys. Rev.* B **56** 9414
[16] Tyagi P and Vedeshwar A G 2001 *Phys. Rev.* B **63** 245315
[17] Alexander W B, Sandoval J and Berg L 2004 *Proc. SPIE* **4540** 106
[18] Turner D E and Harmon B N 1989 *Phys. Rev.* B **40** 10516
[19] Chang Y C and James R B 1992 *Phys. Rev.* B **46** 15040
[20] Howard S T 1994 *J. Phys. Chem.* **98** 6110
[21] Ahuja R, Eriksson O, Johansson B, Auluck S and Wills J M 1996 *Phys. Rev.* B **54** 10419
[22] Ortega F, Caselli E, Lester M and Santiago M 1998 *Phys. Stat. Sol.* (b) **206** R7
[23] Ayres F, Machado W V M, Justo J F and Assali L V C 2003 *Physica* B **340–342** 918
[24] Ayres F, Assali L V C, Machado W V M and Justo J F 2006 *Appl. Phys. Lett.* **88** 011918
[25] Blaha P, Schwarz K, Madsen G K H, Kvasnicka D and Luitz J 2002 *Computer Code WIEN2K* (Vienna University of Technology), improved and updated Unix version of the original [Blaha P, Schwarz K, Sorantin P and Trickey S B 1990 *Comput. Phys. Commun.* **59** 399
[26] Perdew J P, Burke K and Ernzerhof M 1996 *Phys. Rev. Lett.* **77** 3865
[27] Lynch W D In: Palik E D (Ed.) 1985 *Handbook of Opticals Constants of Solids* (New York: Academic Press)
[28] Bassani F and Parravicini G P1975 *Electronic States and Optical Transitions in Solids* (Oxford: Pergamon Press)
[29] Saha S, Sinha T P and Mookerjee A 2000 *Phys. Rev.* B **62** 8828
[30] Murnaghan F D 1944 *Proc. Natl. Acad. Sci.* USA **30** 244
[31] Jeffrey G A and Vlasse M 1967 *Inorganic Chemistry* **6** 396
[32] Wykoff R W G 1963 *Crystal Structures* (New York: Interscience Publishers) Vol. 1
[33] Chester M and Colemann C C 1970 *J. Phys. Chem. Solids* **32** 223
[34] Ahuja R, Eriksson O, Johansson B, Auluck S and Wills J M 1996 *Phys. Rev.* B **54** 10419
[35] Rashkeev S N and Lambrecht W R L 2001 *Phys. Rev.* B **63** 165212
[36] Onida G, Reining L and Rubio A 2002 *Rev. Mod. Phys.* **74** 601
[37] Ouyang C Y, Xiong Z H, Ouyang Q Z, Liu G D, Ye Z Q and Lei M S 2006 *Chin. Phys.* **15** 1585
[38] Jin Y J, Li Z Y and Lin J B 2007 *Chin. Phys.* **16** 506
[39] Kong X L, Hou QY, Qi Y H and Zhi X H 2009 *Acta Phys. Sin.* **58** 4128 (in Chinese)
[40] Lin Z, Guo Z Y, Bi Y J and Dong Y C 2009 *Acta Phys. Sin.* **58** 4128 (in Chinese)
[41] Peng L P, Xu L and Yin J W 2007 *Acta Phys. Sin.* **56** 1585 (in Chinese)
[42] Anedda A, Grilli E, Guzzi M, Raga F and Serpi A 1981 *Solid State Commun.* **39** 1121
[43] Kaneko Y, Morimoto K and Koda T 1983 *J. Phys. Soc. Japan* **52** 4385
[44] Fox M 2001 *Optical Properties of Solids* (New York: Oxford University Press)